ARTICLES

Reliability of Multitaxon, Multiproxy Reconstructions of Environmental Conditions from Accretionary Biogenic Skeletons

Bernd R. Schöne,[1] *David L. Rodland, Jens Fiebig, Wolfgang Oschmann, David Goodwin,*[2] *Karl W. Flessa,*[3] *and David Dettman*[3]

Institute for Geology and Paleontology, INCREMENTS Research Group, Goethe University, Senckenberganlage 32-34, 60325 Frankfurt am Main, Germany
(e-mail: b.r.schoene@em.uni-frankfurt.de)

ABSTRACT

Evaluation and quantification of climate change require data on subseasonal to daily environmental extremes from those periods before instrumental records were available. This study employs a high-resolution, multitaxon, multiproxy approach and analyzes how faithfully accretionary biogenic skeletons record environmental extremes. Six specimens of two bivalve mollusks (*Chione fluctifraga*, *Mytella guyanensi*) and one barnacle species (*Chthamalus fissus*) from a single habitat (northern Gulf of California, Mexico) were collected. Contemporaneous shell portions from these specimens were analyzed for shell growth rates (sclerochronology) and stable isotopes ($\delta^{18}O$, $\delta^{13}C$) and were compared to instrumental records. The results of these analyses included some significant observations. First, shell $\delta^{18}O$ values overestimate winter temperatures and underestimate summer temperatures. Second, the actual diurnal temperature range is not recorded in the biogenic skeletons. Third, skeletal growth is biased toward a species-specific optimum growth temperature (24°–30.9°C). Therefore, higher sampling resolution will not necessarily capture actual environmental extremes. Despite measured temperature extremes of 37.8° and 4.5°C, none of the studied species recorded temperatures above 30.9° or below 12.2°C. Duration and timing of the annual growing period is species specific as well. Faster shell growth occurred at higher temperatures. Up to 58% (*C. fissus*) of the variability in shell growth can be explained by water temperature during growth. Contemporaneous trends in shell $\delta^{13}C$ show a weak correlation with pigment concentration ($R^2 = 0.17$). Higher levels of chlorophyll appear to increase shell production rates. Our study highlights the difficulties inherent in using biogenic skeletons for the reconstruction of paleoenvironmental extremes and demonstrates the power and utility of multiproxy and multitaxon approaches.

Introduction

Subseasonal and daily environmental extremes have recently become a focal point of studies on climate change (Kiktev et al. 2003; Klein Tank et al. 2005). During the past 3 decades, the number of global daily warm temperature extremes has increased more than twice as fast as the corresponding decrease in cold temperature extremes. This resulted in a significant rise in the seasonal temperature spread (Klein Tank and Können 2003). Evaluation and quantification of the anthropogenic impact on climate extremes and seasonality require data from preindustrial times. However, instrumental records of environmental parameters cover only the past 150 yr or so (Jones et al. 2001). Consequently, high-resolution proxy archives of environmental variables would be of great benefit. Such records have been available since the early 1960s. However, in spite of recent theoretical studies (Goodwin et al. 2003; Ivany et al. 2003), it is still barely understood how reliable such proxy records really are.

Manuscript received July 5, 2005; accepted December 12, 2005.

[1] Author for correspondence.
[2] Department of Geosciences, Denison University, 100 Sunset Hill Drive, Granville, Ohio 43023, U.S.A.
[3] Department of Geosciences, University of Arizona, Tucson, Arizona 85721, U.S.A.

[The Journal of Geology, 2006, volume 114, p. 267–285] 0022-1376/2006/11403-0001$15.00

Accretionary biogenic skeletons from many different taxonomic groups provide information on daily paleoenvironmental conditions (Wells 1963; Rhoads and Lutz 1980). Organisms from the intertidal zone, particularly bivalve mollusks (Barker 1964; Evans 1972; Pannella 1976; Richardson et al. 1981) and barnacles (Bourget and Crisp 1975; Killingley and Newman 1983; Achituv et al. 1997), are preferred for such studies because they show distinct tide-controlled growth patterns in their hard tissues, e.g., lunar daily growth increments (LDGIs) and fortnightly tidal bundles. In some early studies, the number and width of daily increments of fossils were used to estimate the changing length of the day and the increasing distance between the earth and the moon through time (Berry and Barker 1968; Rosenberg and Runcorn 1975) or to analyze relative changes of temperature, food, tides, and so forth. (Ansell 1968; Pannella and MacClintock 1968; Berry and Barker 1975; Ohno 1989). Analysis of periodically formed growth structures (sclerochronology) is prerequisite for an absolute dating control of each portion of accretionary biogenic hard parts (Pannella and MacClintock 1968; Evans 1972; Schöne et al. 2002*b*; Goodwin et al. 2003). In this study, LDGIs and fortnightly growth increments of barnacle and bivalve mollusk skeletons were used to temporally contextualize each shell portion and the shell isotope record.

Formation of periodic growth structures involves a complex interplay of genetically determined biological clocks and external pacemakers. In intertidal settings, physiology and growth are closely linked to the periodic rising and falling of the water (Evans 1972; Richardson et al. 1980; Ohno 1989). The tides control and constantly reset the intrinsic biological clocks. According to Palmer et al. (1994), organisms exposed to semidiurnal tides possess two 24.8-h clocks that are linked in antiphase, resulting in 12.4-h, or circalunidian, cycles. Circalunidian clocks enable organisms from such settings to anticipate changing levels of food supply, temperature, and water coverage.

Advanced analytical techniques have permitted quantitative, subseasonal reconstructions of environmental conditions from geochemical properties of the skeletons, especially oxygen isotopes (e.g., Krantz et al. 1987). Many organisms form shell carbonate in oxygen isotopic equilibrium with the surrounding water (Epstein et al. 1953; Mook and Vogel 1968; Wefer and Berger 1991; Hickson et al. 1999) and were hence often used for the reconstruction of seasonal paleotemperature extremes or computation of annual mean temperatures (Weidman et al. 1994; Bice et al. 1996; Marsh et al. 1999; Tripati et al. 2001; Zakharov et al. 2005). However, the potential of growth increment analysis for precise intra-annual calendar alignment of each shell portion, even for single seasons, was neglected in almost all such studies (e.g., Krantz et al. 1987; Khim et al. 2000; Putten et al. 2000; Wurster and Patterson 2001). Thus, their data are of limited use because the timing of shell formation was not recognized.

More recently, theoretical studies combined sclerochronological and isotope geochemical approaches and investigated how precisely environmental data can be extracted from shells of bivalve mollusks. On the basis of extensive modeling, Goodwin et al. (2003) concluded that low spatial sampling resolution and decreasing length of the growing season with increasing ontogenetic age limit the possibility of inferring the full range of seasonal environmental variability. In effect, reduced rates of carbonate production during older life stages attenuate environmental amplitudes (Goodwin et al. 2003; Ivany et al. 2003).

Another consideration is that currently available studies were always based on single species. We are not aware of any study that used different, live-collected, contemporaneous species from the same habitat in combination with each other in order to validate and verify environmental records obtained from a single species.

Here, we analyze a daily-resolution multitaxon record of environmental conditions in conjunction with instrumental records. Reconstructions are based on combined sclerochronological and stable isotope analyses of shell carbonate of two intertidal bivalve mollusk species and one barnacle species from the northern Gulf of California, Mexico. The main questions are as follows: (1) Are some species more suitable for high-resolution environmental studies than others? (2) Can records contained in different species complement each other and improve environmental reconstructions? (3) Can higher sampling resolution really provide a better insight into actual seasonal extremes? Results of our study can increase our ability to interpret climate records from biogenic skeletons.

Material and Methods

The study area is located near the delta of the Colorado River in the northern Gulf of California (fig. 1). Since the construction of upstream dams and diversion of the river during the 1930s, only a trickle reaches the Gulf. As a result, normal marine conditions have prevailed near the delta since that time (Lavín and Sánchez 1999). The study area ex-

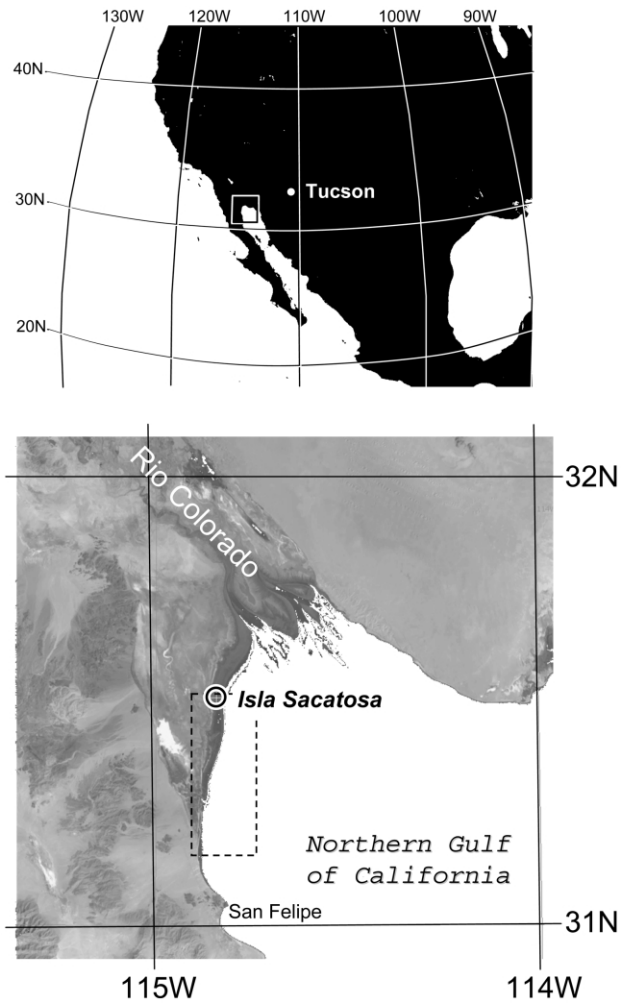

Figure 1. Map showing sample locality (Isla Sacatosa) in the intertidal zone near the mouth of the Colorado River. The small square (*top*) indicates the instrumental (National Centers for Environmental Prediction) temperature data grid used for comparison with the shell data. The dashed rectangle (*bottom*) refers to the SeaWIFS pigment concentration (chlorophyll a) data grid. Map template taken from NASA WorldWind (http://worldwind.arc.nasa.gov/).

periences semidiurnal tides with minimum and maximum heights of about 2 and 5–6 m above mean sea level, respectively. According to satellite measurements (fig. 1; National Centers for Environmental Prediction National Meteorological Center [NCEP-NMC] reanalysis, "skin temperature," i.e., air temperature plus sea surface temperature, centered at 114°37′50E, 31°25′67N, extension: 113°25′80–115°18′60E, 30°28′80–32°22′80N; see http://www.cdc.noaa.gov), temperatures exhibit a huge seasonal variation ranging from +49.05°C during midday in summer to −8.05°C during cold winter nights.

Instrumental Data. A HOBO Temp temperature logger was placed in the intertidal zone approximately 2 m above the mean low-water level near Isla Sacatosa (31°30′35N, 114°50′47W; fig. 1) on December 5, 1999. The logger was affixed to and encapsulated within a plastic container and chained to a concrete anchor. The surface of the protective container was perforated with holes roughly 5 mm in diameter, allowing water to circulate around the logger whenever it was immersed. Ambient temperature was recorded at 5-h intervals (subdaily T_{logger}; fig. 2*A*). Date of recovery was during spring tide on December 9, 2000, at 6:30 a.m., 2 d before the full moon. Although the logger ceased recording on September 7, 2000, we obtained a temperature record of a full year by combining the data with satellite measurement (NCEP-NMC reanalysis).

For calculation of lunar daily temperatures, the logger data were transformed in a new, continuous chronology. Data between successive measurements taken every 5 h were inferred by linear integration. Subsequently, the time series was resampled at 24.8-h (lunar day) intervals using the Macintosh freeware Analyserie, version 1.1 (lunar daily T_{logger}; fig. 2*A*). Following the same procedure, we computed lunar day temperatures from the NCEP-NMC solar day temperature time series (lunar daily T_{NCEP}; fig. 2*B*). Lunar daily NCEP-NMC and logger temperature curves matched each other well and exhibited a highly significant linear correlation ($R = 0.95$, $R^2 = 0.91$, $p < 0.0001$; fig. 2*B*). The linear regression model between logger and NCEP data was used to reconstruct temperatures for the period after the logger had failed (reconstructed lunar daily T_{logger}; fig. 2*B*). Logger temperatures and reconstructed logger temperatures were combined to compute a new lunar daily temperature curve, T_{mm}.

Because the logger fell dry during low tide and recorded air temperatures, we tested whether the T_{mm} record differed significantly from a temperature curve that precludes emersion periods. We used the custom-designed tide calculator of B. Lofgren (University of Arizona) to compute a new lunar daily water temperature curve, T_{mmi} (fig. 2*C*); T_{mm} and T_{mmi} did not reveal significant differences (fig. 2*B*, 2*C*; $R^2 = 0.97$, $p < 0.0001$). Daily temperature extremes and interdaily temperature fluctuations were exaggerated by the T_{mmi} data because the T_{mmi} curve consists of fewer data points than that of T_{mm}. We thus relied on using the more complete T_{mm} record for comparison with shell growth and isotopes in this study. Still, subdaily temper-

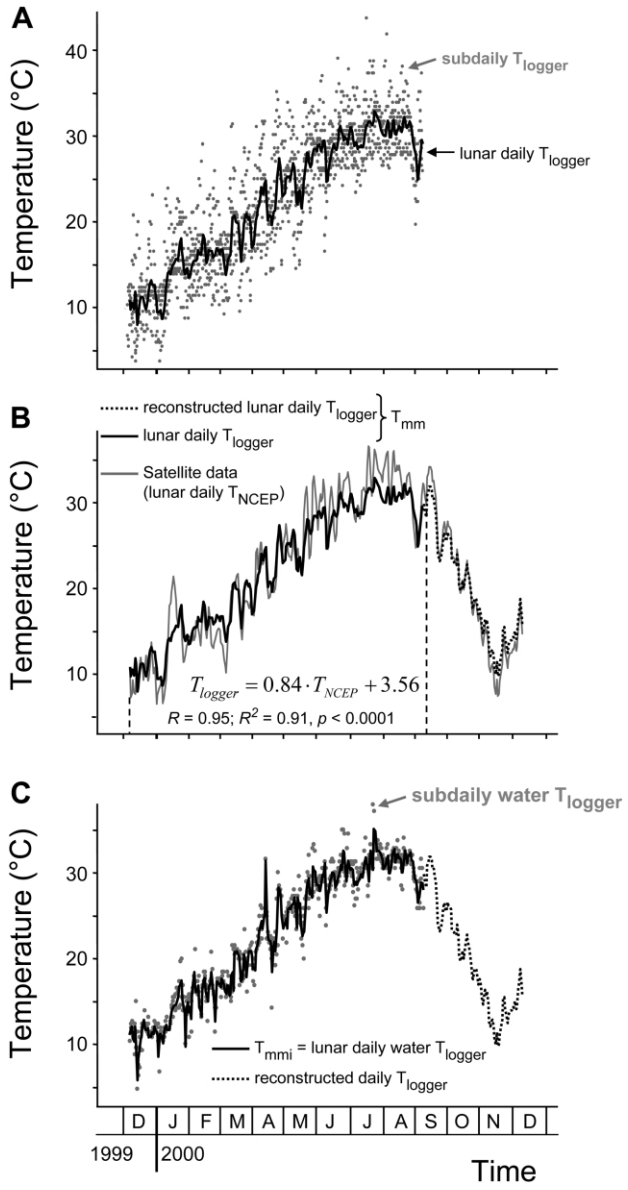

Figure 2. Temperature data. *A*, Temperature (T_{logger}) recorded at 5-h intervals by a logger deployed approximately 2 m above the mean low-water level near Isla Sacatosa (31°30′35N, 114°50′47W; fig. 1). These data were transformed into lunar daily (24.8-h) temperatures. *B*, Satellite-derived (solar, 24-h) daily temperatures (T_{NCEP}; National Centers for Environmental Prediction [NCEP]), converted into lunar daily temperatures, were used to reconstruct T_{logger} data (*dotted curve*) for times when the logger failed in its recording. The measured and reconstructed T_{logger} data were combined into a new series, T_{mm}. Only T_{mm} values during submersion (high tide) are shown, T_{mmi}. Note that subdaily water temperatures exceed 35°C during summer. The T_{mmi} curve does not differ significantly from that of T_{mm}.

atures that were recorded during submersion (the basis for constructing T_{mmi}) were useful means to determine how water temperatures fluctuated during one lunar day. At the end of July 2000, maximum water temperatures of 37.8°C occurred during midday. Nighttime water temperatures, however, were more than 7°C colder, 30.3°C. During mid-December, subdaily water temperatures ranged from 12.1° (midday) to 4.5°C (midnight).

For estimation of the effects of primary productivity on shell carbon isotopes and shell growth rates, data on pigment concentration in the upper ocean were obtained from NASA/Goddard Space Flight Center (http://www.nasa.gov/goddard). We used weekly data (Level 3 8-Day Standard Mapped Image) on chlorophyll *a* concentration collected by the Sea-viewing Wide Field-of-view Sensor (SeaWiFS) mounted on the Orbview-2 satellite. Spatial coverage is from 31°09′43N–114°25′02W to 31°30′524N–114°44′47W (fig. 1).

When recovered in early December 2000, both loggers were encrusted with several dozen buckshot barnacles (*Chthamalus fissus*; Darwin 1854) of approximately equal size. Their basal plates measured about 1 cm in diameter. We also found one mussel (*Mytella guyanensis*; Lamarck 1819) affixed with its byssus threads to the inner surface of the plastic container containing the temperature logger. Near the logger, five clams (*Chione fluctifraga*; Sowerby 1853) of shell heights between ca. 1.2 and 6 cm were collected alive. For this study, three arbitrarily selected barnacles, one mussel, and two clams were used.

Sample Preparation. After removal of the soft parts, all specimens were cleaned in 5.25% NaOCl to dissolve remaining organic matter, rinsed in deionized water and 99.5% ethyl alcohol (EtOH), and allowed to air-dry. Specimens then were mounted on Plexiglas cubes, and a protective layer of JB KWIK metal epoxy was applied to the surfaces of the shells.

From each bivalve shell, we cut two cross sections along the axis of maximum growth. Barnacles were cross-sectioned through the parietes (shell plates; fig. 3). All slabs were mounted on glass slides with the "mirroring" sides facing up and were thereafter ground (800- and 1200-grit SiC powder) on glass plates and polished (1 μm Al_2O_3 powder) on a Buehler G cloth. After the samples were rinsed ultrasonically in deionized water, the polished surfaces were cleaned with 99.5% EtOH.

Sclerochronology. In order to resolve internal microgrowth patterns, one polished cross section from each specimen was immersed in Mutvei's solution for 23 min at 37°–40°C with constant stirring. Mut-

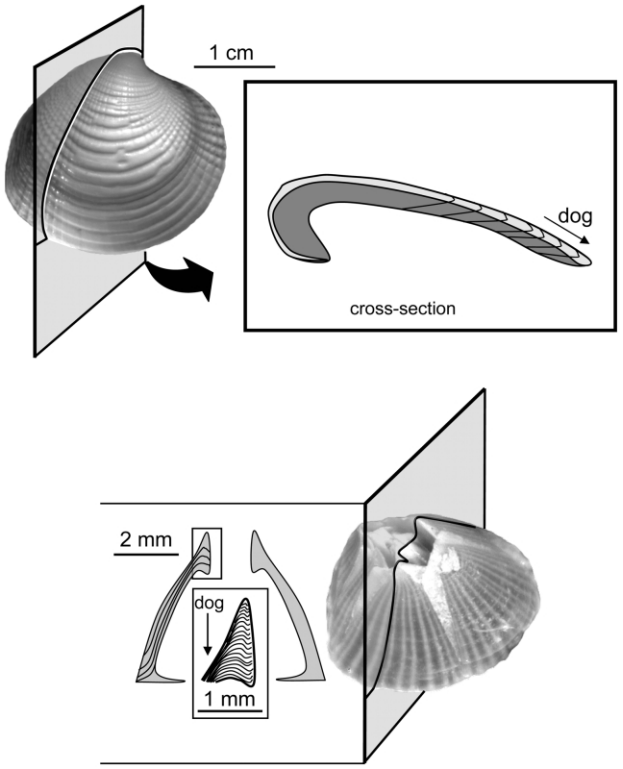

Figure 3. For analysis of internal growth structures, shells of bivalve mollusks and barnacles were cut along the axis of maximum growth. In barnacles, the sheath layer (*inset*) was studied. *dog* = direction of growth.

vei's solution (Schöne et al. 2005*a*) consists of 0.5% acetic acid, 12.5% glutaraldehyde, and ca. 5–10 g alcian blue/L of solution. This agent simultaneously etches the carbonate, fixates the organic matrix, and stains mucopolysaccharids, thereby increasing the visibility of the microgrowth structures. Immediately after immersion, the samples were carefully rinsed in deionized water and air-dried.

Sections treated with Mutvei's solution were viewed under a binocular microscope at magnifications of 30× to 150× and were digitized with a Nikon Coolpix 995 camera (fig. 4). The custom-designed image-processing software Panopea was used for counting microgrowth increments and measuring their width. In bivalves, we focused on the outer shell layer, while in barnacles, we studied microgrowth structures of the sheath layer (figs. 3, 4).

For spectral analyses, growth trends were removed from the measured microgrowth data by fitting stiff cubic splines to the chronologies (e.g., Cook and Kairiukstis 1990). Continuous wavelet transforms (CWTs; using zero padding to adjust for edge effects, Morlet wavelet, wave number = 8) were computed from residuals of the microgrowth time series. The CWTs reveal inherent frequencies of time series and determine their strength and evolution through time.

Stable Isotope Geochemistry. The mirror-image cross-sectioned slabs were used for the extraction of carbonate powder samples for oxygen and stable carbon isotope analyses. Before sampling, epoxy resin, periostracum, and secondary shell layers were mechanically removed. Following the shape of the microgrowth increments, aragonite or high-Mg calcite (HMC) powder was milled (see fig. 4 in Schöne et al. 2005*b*) from the outer shell layer of the bivalves or the sheath layer of the barnacles, using a cylindrical diamond-coated drill bit (1-mm diameter). A total of 179 individual millings were completed (table 1). Each milling step parallel to the direction of growth measured between ca. 100 and 450 μm perpendicular to the growth direction and yielded about 60 μg of carbonate powder. For the bivalves, this corresponded to a temporal resolution of about <1 d to 1 wk per sample. Two of the barnacles (ST11-A6 and ST11-A7) were sampled with a resolution of 4 d to 3 wk. Samples were analyzed with a Finnigan MAT 253 continuous-flow mass spectrometer equipped with a Gas Bench II. Isotope values are reported relative to Vienna Pee Dee Belemnite (VPDB) on the basis of an NBS-19 value of −2.20‰ for $\delta^{18}O$ and 1.95‰ for $\delta^{13}C$. On average, replicated precision (multiple measurements of the NBS standard) was better than 0.07‰ (1 SD) for $\delta^{18}O$ and better than 0.05‰ (1 SD) for $\delta^{13}C$.

Oxygen isotope ratios of calcium carbonate were used to reconstruct water temperatures [$T_{\delta^{18}O}$]. For the aragonitic skeletons of *C. fluctifraga* and *M. guyanensis*, we used the paleothermometry equation of Grossman and Ku (1986). A small modification of their equation was required because they report water values in standard mean ocean water (SMOW: 0.2‰; Goodwin et al. 2001). The corrected function is

$$T_{\delta^{18}O(\text{aragonite})} = 20.60 - 4.34 \times [\delta^{18}O_{\text{aragonite}} - (\delta^{18}O_{\text{seawater}} - 0.20)]$$

where $T_{\delta^{18}O(\text{aragonite})}$ is measured in degrees Celsius. As in other barnacles, the skeleton of *C. fissus* consists of HMC. We used the paleotemperature equation by Killingley and Newman (1983) to recon-

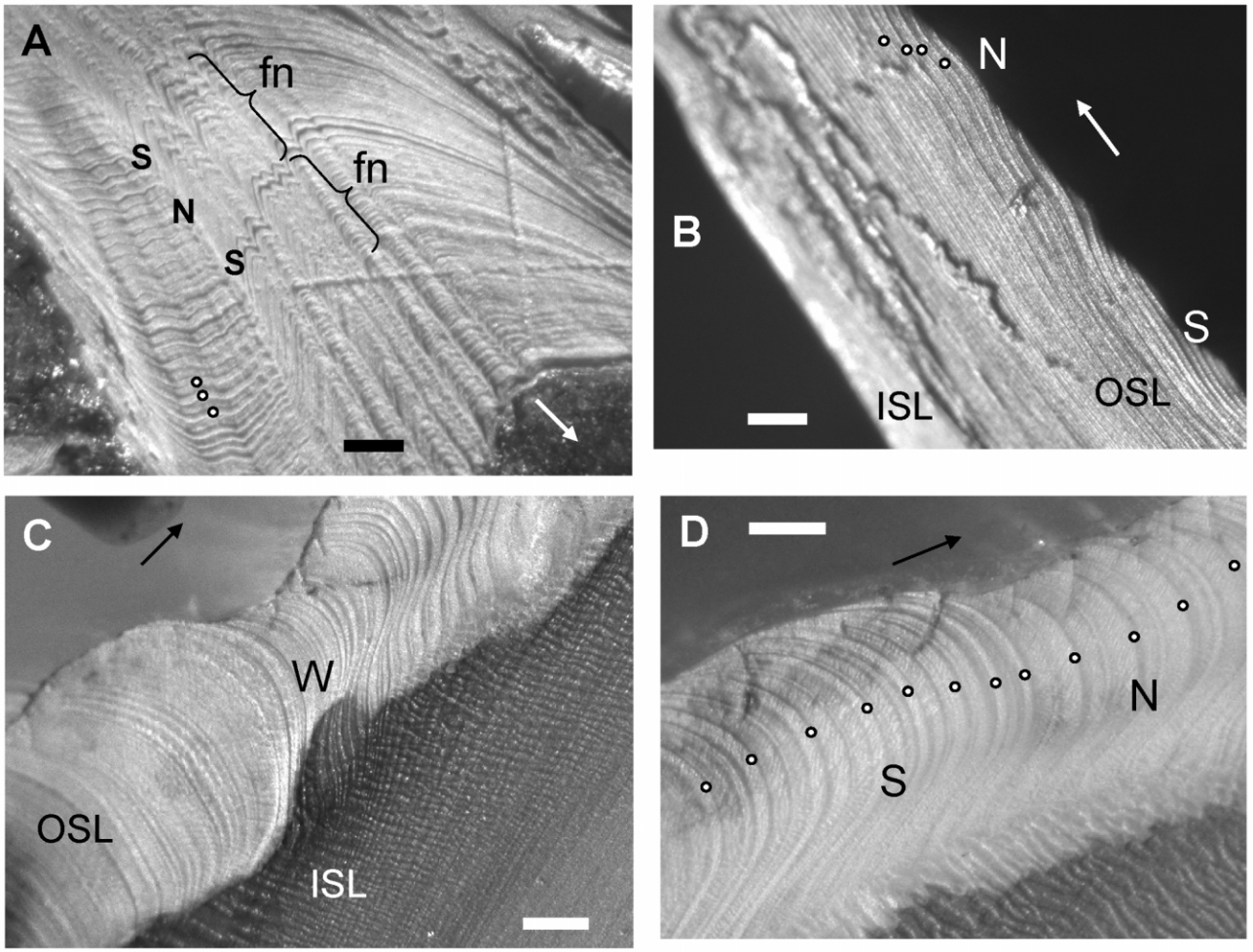

Figure 4. Growth patterns after immersion in Mutvei's solution. *Arrow* = direction of growth; *circles* = lunar daily growth increments (LDGIs); *N* = neap tide; *S* = spring tide; *ISL* = inner shell layer; *OSL* = outer shell layer. *A*, Sheath layer of *Chthamalus fissus* (ST11-A7). LDGIs are arranged in fortnight bundles (*fn*). Scale bar = 100 μm. *B*, LDGIs in *Mytella guyanensis* (ST11-A5L) approach OSL at a very low angle. Scale bar = 200 μm. *C*, Winter break (*W*) in *Chione fluctifraga* (ST11-A2L). Scale bar = 200 μm. *D*, Tide-controlled LDGI pattern in *C. fluctifraga* (ST11-A2L). Daily increments formed during neap tide are broader than those formed during spring tide. Spring tide LDGIs show distinct semidiurnal microgrowth lines. Scale bar = 200 μm.

struct ambient water temperature during formation of the skeleton:

$$T_{\delta^{18}O(HMC)} = 22.14 - 4.37 \times (\delta^{18}O_{HMC} - \delta^{18}O_{seawater}) + 0.07 \times [(\delta^{18}O_{HMC} - \delta^{18}O_{seawater})^2],$$

where $T_{\delta^{18}O(HMC)}$ is measured in degrees Celsius, $\delta^{18}O_{aragonite}$ and $\delta^{18}O_{HMC}$ are measured relative to the VPDB scale, and $\delta^{18}O_{seawater}$ is measured relative to the SMOW scale. Thus, assuming no change in $\delta^{18}O_{seawater}$, a 1‰ shift in $\delta^{18}O_{aragonite}$ reflects a temperature change of the ambient sea water of 4.34°C. The relation between temperature and the oxygen isotope composition of the barnacle skeleton is nonlinear. Between +3‰ and −3‰ (=observed range of $\delta^{18}O_{HMC}$ in this study), a shift of the $\delta^{18}O_{HMC}$ value by 1‰ coincides with a temperature change of 4.02°–4.72°C.

Results

Skeletal hard parts of all specimens analyzed in this study experienced semidiurnal tides and showed typical microgrowth (micrometer-scale) patterns

Table 1. Statistics Based on Lunar Daily Growth Increments and Stable Carbon and Oxygen Isotopes of Shells

Species and specimen ID	No. isotope samples	Average spatial resolution (lunar days)	No. measured LDGIs	LDGIs (μm)	$\delta^{18}O$ (‰)	$T_{\delta^{18}O}$ (°C)	$\delta^{13}C$ (‰)
Barnacles:							
Chthamalus fissus:							
ST11-A6	17	5.3	141	21, 47, 6	.87, 2.37, −1.92	18.5, 30.8, 12.2	.75, 1.25, −.45
ST11-A7	13	7.1	101	26, 55, 10	.83, 2.22, −1.01	18.7, 26.6, 12.8	.44, .85, −.38
ST11-A8	4	17.3	119	22, 47, 8	1.52, 2.27, .31	15.7, 20.8, 12.6	NA
Bivalve mollusks:							
Mytella guyanensis:							
ST11-A5L	81	1.2	80	321, 952, 86	−1.03, 1.27, −2.45	24.2, 30.4, 14.2	.47, .85, −.07
Chione fluctifraga:							
ST11-A2L	23	6.7	155	54, 195, 11	−.67, .78, −2.06	22.6, 28.7, 16.3	−.17, .58, −.97
ST11-A3L	41	3.8	157	72, 190, 14	−1.30, 1.10, −2.57	25.4, 30.9, 15.0	.04, .73, −1.01

Note. Temperatures were reconstructed from shell $\delta^{18}O$ values using the paleothermometry equation of Grossman and Ku (1986) for aragonitic shells of the bivalve mollusk, and the equation of Killingley and Newman (1983) for high-Mg calcite of the barnacles. Values for lunar daily growth increments (LDGIs), $\delta^{18}O$, $T_{\delta^{18}O}$, and $\delta^{13}C$ are shown as mean, maximum, and minimum. NA = not available.

typical for organisms from the intertidal zone, namely, LDGIs (fig. 4; Goodwin et al. 2001; Schöne et al. 2002*a*, 2002*b*). LDGIs consist of couplets of two semidiurnal microgrowth increments that are separated by alternating thin and thick microgrowth lines arranged in fortnight bundles (fig. 4*A*, 4*D*). During each fortnight period, maximum shell growth rate was associated with neap tides and minimum rate with spring tides. Thin microgrowth lines were present at the ventral margin of all specimens when collected on the morning of December 9, 2000. These lunar daily and fortnightly growth patterns assisted in adding a relative time axis to the isotope geochemical record of the skeletons. Furthermore, cross-dating of the temporally aligned $T_{\delta^{18}O}$ curves and instrumental temperature measurements enabled a precise calendar dating of each shell portion.

Calendar Alignment of the Growth and Isotope Records. Hard parts of the barnacles, mussel, and clams formed at different times of the year (fig. 5). While the barnacles apparently grew without major growth halts after settling on the surface of the temperature logger encasement, bivalve growth was interrupted for periods of several weeks.

The sheath layers of the three specimens of *Chthamalus fissus* were composed of 101–141 LDGIs (table 1). Major growth lines (e.g., annual growth breaks) were not observed. We arranged the sclerochronological records so that the last LDGI coincided with the date of collection (i.e., December 9, 2000; fig. 5*A*–5*C*). The sclerochronologically aligned $T_{\delta^{18}O(HMC)}$ records compared very well with the instrumental daily temperature chronology T_{mm}. The LDGI counts reveal that the balanomorphs started growing shell on July 17 (ST11-A6; fig. 5*A*), August 28 (ST11-A7; fig. 5*B*), and August 9, 2000 (ST11-A8; fig. 5*C*). Dating precision (± 10 LDGIs) is limited by the sampling resolution for shell isotopes (time averaging).

The growth record of the mytiloid bivalve *Mytella guyanensis* was more difficult to align than those derived from barnacles (fig. 5*D*). As before, LDGI counts provided temporal context for the isotope data. However, in umbonal shell portions, growth structures were not identifiable. Only the most recently formed 80 LDGIs could be counted and their widths determined. For shell portions without sclerochronological dating control, it was assumed that the time represented by each individual isotope sample was comparable to that of similar isotope samples where measurable microgrowth increments were present.

A distinct major growth line indicative of a growth interruption was observed approximately eight LDGIs away from the ventral margin. On the basis of comparison with temperature data, these eight LDGIs were probably formed during early December. We arranged the remaining $T_{\delta^{18}O(aragonite)}$ curve so that the last $T_{\delta^{18}O(aragonite)}$ value immediately before the growth break coincided with the water temperature before the coldest season of the year (i.e., October 23, 2000). Sclerochronologically aligned $T_{\delta^{18}O(aragonite)}$ before that date almost perfectly matched the measured water temperature T_{mm} (fig. 5*D*). Although absolute temperatures were underestimated by the $\delta^{18}O_{aragonite}$ values, both curves exhibited a high running similarity. If the calendar alignment is correct, *M. guyanensis* started growing shell during the hot summer at around July 15,

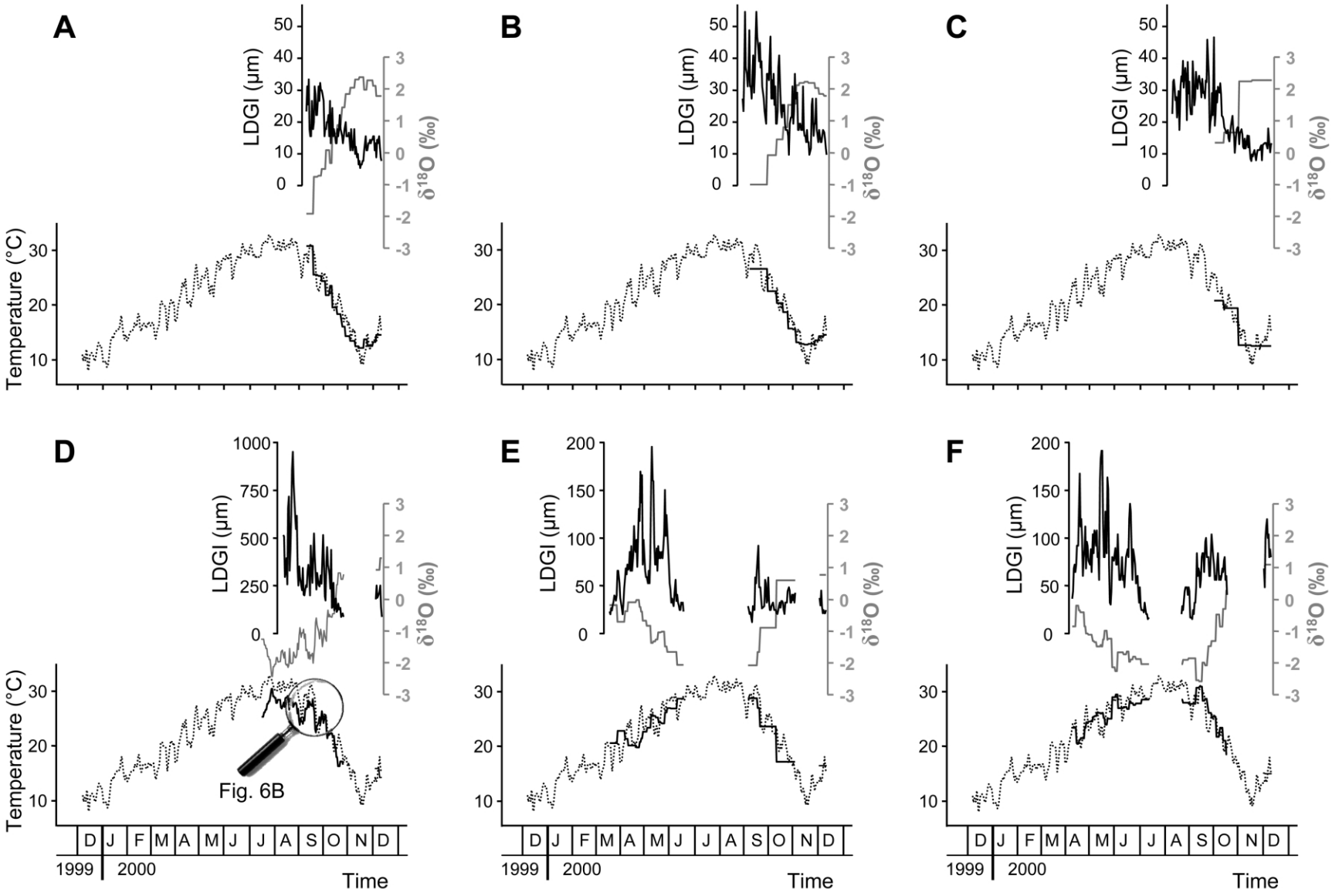

2000. However, no appreciable amounts of carbonate were deposited between October 24 and December 1, 2000.

The calendar alignment of the shell growth and isotope record of *Chione fluctifraga* was hampered by the presence of two seasonal growth interruptions. These were described in detail by Schöne et al. (2002*a*): a dark winter growth line (fig. 4*C*) and a purple zone indicating slowdown and subsequent interruption of growth during the hot summer. LDGIs and shell isotopes were measured between the penultimate winter line and the ventral margin. Despite differences in ontogenetic age, both specimens exhibited almost exactly the same length of growing season. We counted 155 LDGIs in specimen ST11-A2L (years 2–3) and 157 LDGIs in the third and the beginning of the fourth year of growth in specimen ST11-A3L (table 1).

Each shell record was divided into three segments separated by the winter and summer lines (fig. 5*E*, 5*F*). Wiggle-matching of the $T_{\delta^{18}O(aragonite)}$ and temperature time series (T_{mm}) enabled a precise calendar alignment of these growth segments. Because of the high spatial sampling resolution for isotope analyses (in most shell portions, between two and nine LDGIs per powder sample), we were able to recognize fortnight periods in the $T_{\delta^{18}O(aragonite)}$ record that coincided well with the fortnight periods of the temperatures. This facilitated the calendar alignment of the growth record. In specimen ST11-A2L (fig. 5*E*), the first shell segment between the penultimate winter line and the last purple zone formed between March 19 and June 17, 2000, the following shell portion (purple zone–last winter line) between September 8 and November 5, and the remaining shell segment after the last winter line grew from December 1. The corresponding shell portions of specimen ST11-A3L grew at slightly different times (fig. 5*F*): April 9–July 12, August 27–October 22, and November 30–December 9. Calendar dating may be off by a maximum of 11 LDGIs for specimen ST11-A2L but by only 4.5 LDGIs for ST11-A3L.

Intra- and Interspecific Comparison of Shell $\delta^{18}O$ Values. Regardless of the sampling resolution, $T_{\delta^{18}O}$ curves of all specimens and species matched each other quite well (fig. 6*A*). The highest temporal resolution during the summer was 0.5 to two lunar days in bivalves and three lunar days in barnacles (table 1), while the average sampling resolution was about 1.2–7.1 lunar days. The average difference of reconstructed temperature among different specimens was less than ca. 2°C. Deviation between the $T_{\delta^{18}O}$ curves of different taxa increased toward higher temperatures. Irrespective of higher water temperature, shell carbonate of bivalves and barnacles did not record temperatures >30.9°C.

Mytella guyanensis was the only organism studied here that formed carbonate during the hottest part of the summer (fig. 6*A*). The maximum temperature recorded by its shell $\delta^{18}O_{aragonite}$ values did not exceed 30.4°C. But its instrumentally recorded daily (average) temperature during this period was up to 2°C higher. The most extreme instrumentally recorded subdaily water temperatures, however, were up to 7.4°C higher. Furthermore, subdaily sampling resolution did not increase the maximum $T_{\delta^{18}O}$. As demonstrated in figure 6*B*, subdaily $T_{\delta^{18}O}$ (one-half LDGI = one high-tide cycle, approximately 6 h in duration) of *M. guyanensis* ranged near the lower subdaily water temperature extreme. Mean daily temperatures from $\delta^{18}O_{aragonite}$ values were underestimated by 2.7°C.

Generally, *C. fissus* recorded actual daily temperatures during the warm season more reliably than the bivalves (fig. 6*A*). The warmest recorded $\delta^{18}O_{HMC}$-based temperatures differed from instrumentally determined daily temperatures only by a few fractions of a degree centigrade (T_{mmi} = 12.1° and 31.1°C, $T_{\delta^{18}O(HMC)}$ = 12.2° and 30.8°C, respectively).

Cold temperatures limited shell growth of the bivalve mollusks (fig. 6*A*). Bivalve mollusks did not form new shell during the cold season of the year, when daily temperature fell below 14.2°C (*M. guyanensis*) and 15°C (*C. fluctifraga*). Although barnacles grew during the entire cold season, minimum temperature reconstructed from their shell oxygen isotopes (12.2°C) overestimated the actual daily water temperature by at least 3°C and the most extreme winter temperatures by 7.7°C.

Intra- and Interspecific Comparison of Growth Rates. Specimens from different species exhibited large differences in their absolute skeletal growth

Figure 5. For calendar alignment of the lunar daily growth increments (LDGIs), oxygen-isotope-derived temperatures (*solid lines*) were compared with instrumental temperature curves (T_{mm}; *dotted lines*). *A–C*, *Chthamalus fissus*. *A*, ST11-A6. *B*, ST11-A7. *C*, ST11-A8. *D*, *Mytella guyanensis*, ST11-A5L. *E*, *F*, *Chione fluctifraga*. *E*, ST11-A2L. *F*, ST11-A3L.

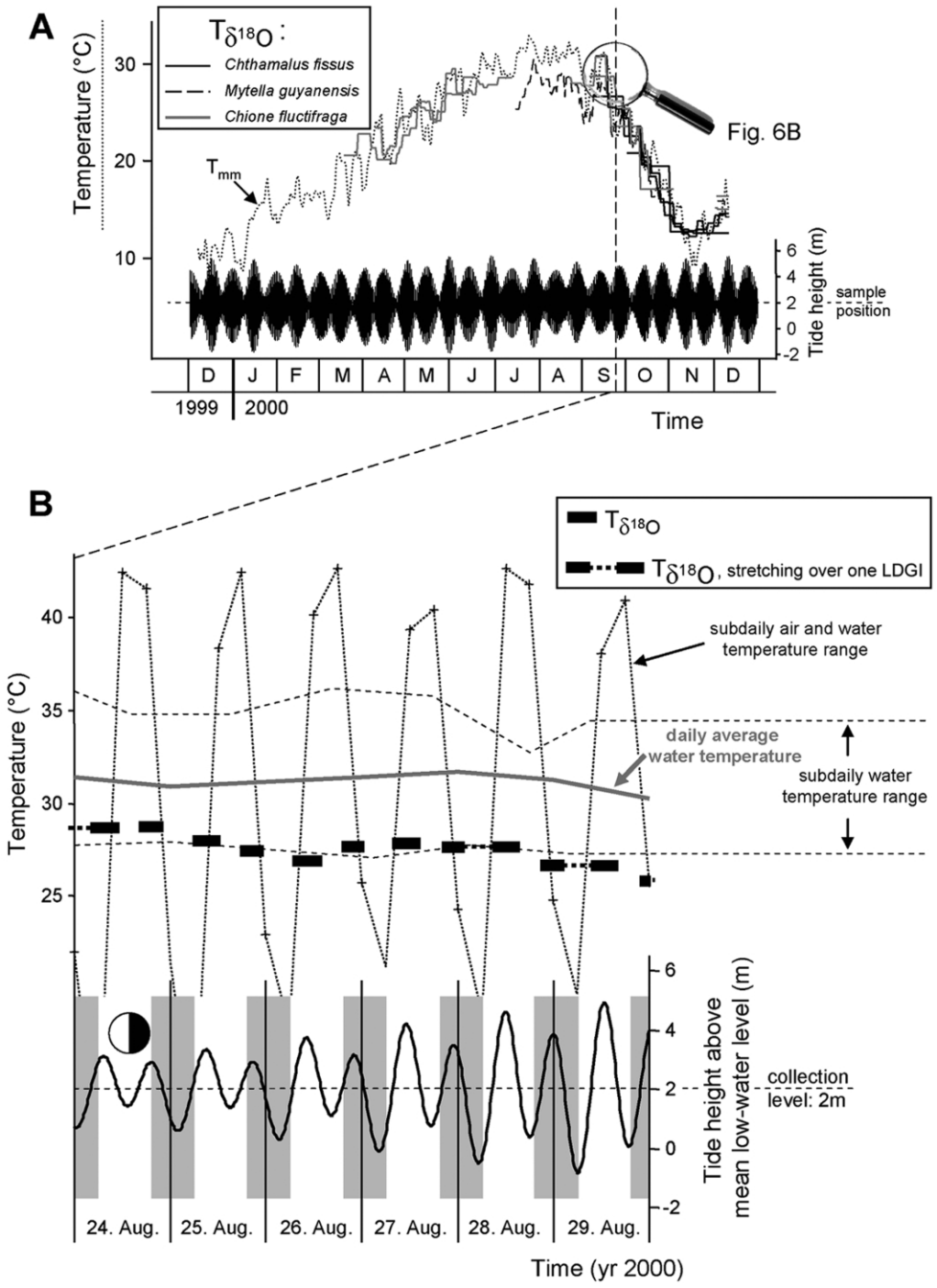

Figure 6. Reconstructed (shell $\delta^{18}O$) and instrumentally determined (T_{mm}) temperatures. *A*, $T_{\delta^{18}O}$ curves of the different specimens exhibit good agreement with each other and with T_{mm}. Actual water temperatures are underestimated during the hottest part of the summer and overestimated during winter by $T_{\delta^{18}O}$. The warmest temperatures during each fortnightly tidal cycle occur during neap tides (visible in T_{mm} and $T_{\delta^{18}O}$). *B*, Enlarged portion of *A* showing a subdaily $T_{\delta^{18}O}$ record of *Mytella guyanensis*. Note that $T_{\delta^{18}O}$ closely follows the lower range of T_{mm}. Apparently the shell did not grow during extreme temperatures. Shell growth occurred preferentially at optimal growth temperatures.

rates. However, irrespective of their taxonomic identity, all specimens grew faster during warmer temperatures. Furthermore, they showed higher growth rates during neap tides than during spring tides (fig. 4*A*, 4*B*, 4*D*). Remarkably similar rates of skeletal accretion were observed among specimens of the same species and similar ontogenetic age (fig. 7*A*).

During their first year of growth, *C. fissus* accreted on average 21–26 μm of carbonate to the sheath layer every lunar day. Shell growth reached maximum rates of 55 μm per lunar day during September and then continuously decreased toward December. Minimum LDGI widths (6 μm) were found in shell portions deposited during mid-November. Continuous wavelet analysis revealed strong spectral power at periods of approximately 14 LDGIs, most pronounced during the first 2 mo of growth (fig. 7*B*).

The mytiloid bivalve mollusk, *M. guyanensis*, exhibited the fastest growth rates of all studied species (on average 321 μm). During its first summer, the mussel accreted almost 1 mm of carbonate to its shell every lunar day. Minimum growth rates were associated with the cold season of the year (86 μm/LDGI during November).

Shells of *C. fluctifraga* grew about five times slower than those of the mussel. Average increase in shell height was 54–72 μm in the 2- and 3-yr-old specimens, while maximum and minimum daily growth rates were about 200 and 15 μm, respectively, in both shells. Fortnight cycles are well expressed (fig. 7*C*).

Relation between Skeletal Growth and Temperature. Logarithmic regression analyses revealed strongly positive correlations between water temperature ($T_{\delta^{18}O}$) and shell growth of *M. guyanensis* and *C. fissus* (fig. 8); 51%–58% of the variability in LDGI width of the mussel and the buckshot barnacles can be explained by ambient water temperature (fig. 8*A*–8*D*). The fastest growth rates occurred at 28.5°C in *M. guyanensis* and at ca. 30°C in *C. fissus*.

The $T_{\delta^{18}O}$ plots of *C. fluctifraga* showed the typical growth temperature optimum (Goodwin et al. 2001; Schöne et al. 2002*a*) at ca. 24°–27°C (fig. 8*E*, 8*F*). Higher and lower temperatures resulted in strongly reduced shell growth. A rational function is most suitable to describe the growth-temperature relation. The R^2 values are lower than for the mussel and barnacles: 0.27 (ST11-A3L; $R = 0.52$) and 0.15 (ST11-A2L; $R = 0.39$).

Shell stable carbon isotope ratios. Despite discrepancies of up to 1‰ in contemporary shell portions, barnacles, and bivalve mollusks showed some common trends in carbon isotopes (fig. 9*A*). Shell carbon isotope values reveal weak linear covariance with weekly pigment concentration data ($R^2 = 0.18$, $R = 0.42$, $p = 0.05$; fig. 9*B*). While pigment concentration and shell carbon isotopes were closely related to each other during spring and summer, the curves diverged distinctly from September through December. In general, shell $\delta^{13}C$ values became more positive toward early summer (+0.71‰ in *C. fluctifraga*, +0.85‰ in *M. guyanensis*). After a sudden shift toward more negative values in September (+0.08‰ in *M. guyanensis*, −1.01‰ in *C. fluctifraga*), shell $\delta^{13}C$ values reached a maximum in late October and early November (up to +1.25‰ in *C. fissus*). Carbon isotope values more depleted in ^{13}C were measured in December 2000 (most extreme values: −0.94‰ in *C. fluctifraga*, +0.10‰ in *M. guyanensis*; table 1).

The $\delta^{13}C_{aragonite}$ curves of the two *C. fluctifraga* specimens were quite similar during the first half of the year. At maximum, $\delta^{13}C_{aragonite}$ values differed by 0.5‰. However, the curves had little in common after the hot summer (−0.97‰ in ST11-A2L, +0.73‰ in ST11-A3L). Specimen ST11-A3L followed more closely the $\delta^{13}C$ values of the barnacle ST11-A7 and the mussel. Intraspecies discrepancies were also observed in the $\delta^{13}C_{HMC}$ values of the barnacles. Despite almost exactly the same ontogenetic age, carbon isotope ratios in shell portions of ST11-A6 and ST11-A7 differed by up to almost 1‰ in mid-September (+0.31‰ in ST11-A6 vs. +1.24‰ in ST11-A7).

Discussion

Combined sclerochronological and isotope geochemical analyses of accretionary skeletons from different contemporaneous species can be used for a variety of different purposes, such as studies on population dynamics, life histories, and so forth. Multitaxon, multiproxy approaches can also greatly improve environmental reconstructions.

Advantages of Multitaxon Environmental Reconstructions. Calendar-aligned oxygen-isotope-derived temperature curves of specimens belonging to different taxa from the same habitat compared well with each other and with instrumental measurements. Apparently, shell carbonate of *Chthamalus fissus*, *Mytella guyanensis*, and *Chione fluctifraga* was deposited in close oxygen-isotopic equilibrium with the surrounding seawater. Furthermore, despite large subdaily swings in instrumentally determined water temperature of almost 8°C, the different taxa exhibited only minor variability in the recorded temperature (fig. 6*A*). This leads to the

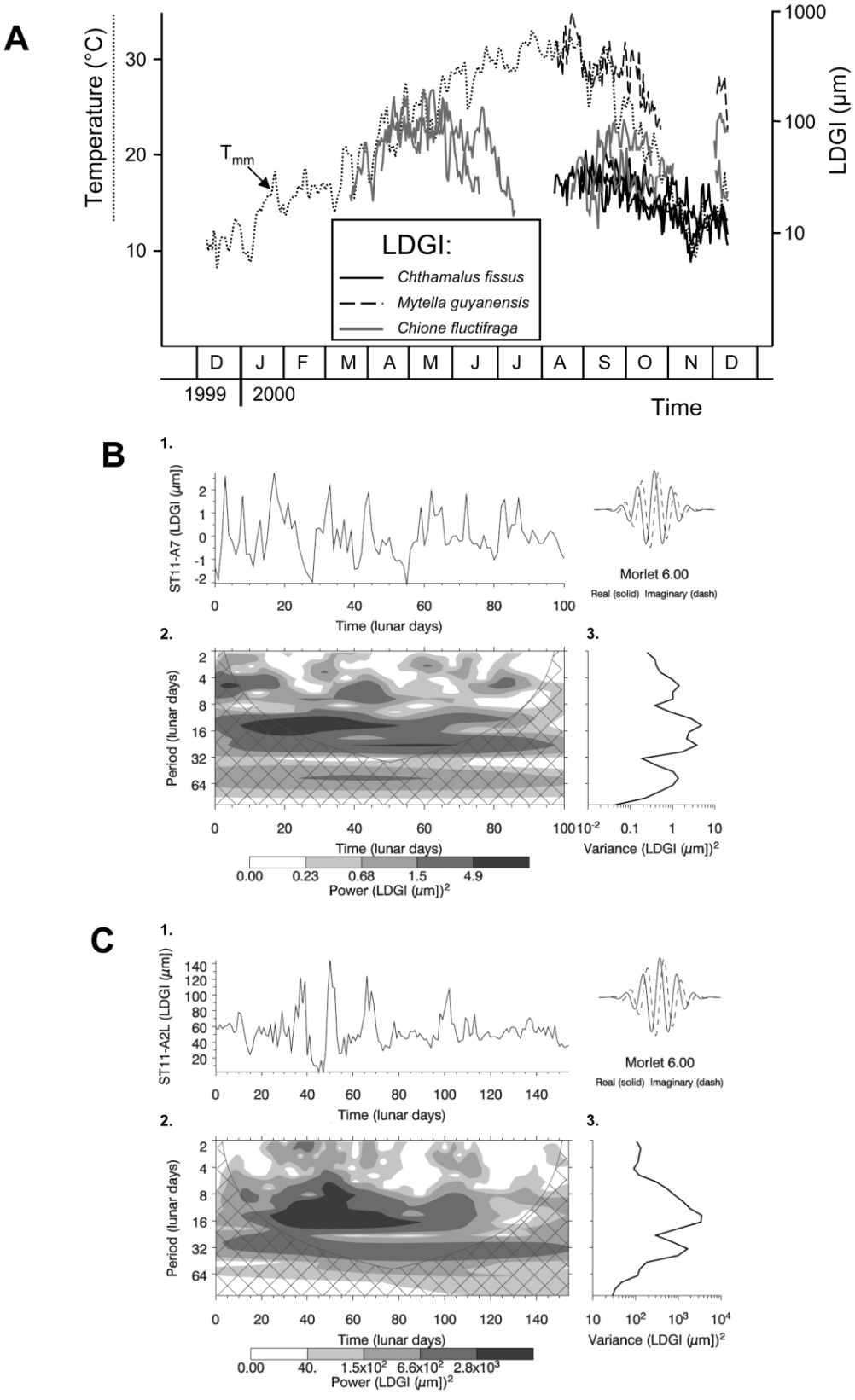

conclusion that no significant differences occurred among the different species in the timing of skeletal growth during each submersion period.

The integrated analyses of proxy records from various species enabled cross-validation and cross-verification of environmental reconstructions. As shown for other invertebrate skeletons, particularly bivalve mollusks (Ansell 1968; Hall et al. 1974; Clark 1979; Jones and Quitmyer 1996), the timing of the annual growing period and temperature thresholds are species specific. None of the three species studied here provided a complete year-round record of environmental variables (figs. 5, 6). Nevertheless, the different records complemented each other, and gaps in the record of one species were bridged by records of another species.

In addition, growth rates were much higher in *M. guyanensis*. Faster shell growth results in broader growth increments and, therefore, higher spatial and temporal resolution (fig. 6*B*). Whereas growth rates of *C. fissus* were generally very low and sampling for shell isotopes was difficult, *C. fluctifraga* grew particularly slowly during the hot summer. As seen from growth-temperature plots, *M. guyanensis* exhibited maximum accretion rates during the same time interval. However, fast shell growth comes with one disadvantage: growth increments and lines approach the outer shell surface at a very low angle. This is true for many other mytiloid bivalves such as *Mytilus edulis* (Linnaeus 1758) or *Semimytilus algosus* (Gould 1850; e.g., Abades et al. 2000). Growth lines and increments in the shell of *M. guyanensis* are arranged in a roof-tile-like structure, and only a limited number of LDGIs can be viewed at once. This makes identification of fortnight bundles in the shell of *M. guyanensis* more complicated than in *C. fluctifraga* and *C. fissus*.

Limitations of Environmental Reconstructions Based on Biogenic Hard Parts. Despite annual curves matching nicely, the daily temperature curves reconstructed from shell oxygen isotopes from different species did not. However, we did not expect a perfect match for the following reasons: (1) the precision of oxygen isotope measurements was about 0.07‰ (1 SD), implying an error in temperature estimates of ca. ±0.3°C; (2) spatial sampling resolution for shell isotopes differed from one sample to the next; (3) temperature was not recorded during periods of nongrowth, i.e., during low tide and aerial exposure; and (4) maximum carbonate production occurred at a species-specific optimum temperature range. For example, *C. fluctifraga* grew at the fastest rates between 24° and 27°C, while *M. guyanensis* and *C. fissus* were fastest at warmer temperatures of about 29°C.

As observed for other bivalves (Goodwin et al. 2001; Schöne et al. 2002*a*), none of the species analyzed here provided a perfect record of the actual annual temperature range. None of the studied species recorded temperatures higher than 30.9°C. This is true even for *M. guyanensis*, which was sampled at subdaily resolution in some shell portions (fig. 6*B*). Although instrumentally determined daily temperatures were over- and underestimated, daily summer $T_{\delta^{18}O}$ values were within the (lower) range of actual temperatures that occurred during one LDGI (fig. 6*B*). This suggests that shells did not grow at constant rates during the day. Shell growth was interrupted during aerial immersion during low tides and was strongly reduced or even halted during extreme temperatures. Previous studies have demonstrated that bivalves precipitate carbonate preferentially at a narrow optimum growth temperature range (Ansell 1968; Tanabe 1988; Tanabe and Oba 1988; Schöne et al. 2002*b*). Temperature reconstructions can be biased toward optimal growth temperatures. Growth-temperature plots of the three studied species support this hypothesis. It seems possible that summertime shell growth of *M. guyanensis* occurred preferentially during the night and that wintertime shell growth of *C. fissus* occurred during the day. The model in figure 10 schematically describes the relation between preferred shell growth at optimal growth temperatures

Figure 7. *A*, Lunar daily growth increment (LDGI) curves and water temperature (T_{mm}). Daily growth rates of the same species compare well with each other. *Mytella guyanensis* grew at the fastest rates of all studied specimens. *B*, *C*, Continuous wavelet spectra (ION script at http://www.researchsystems.com; after Torrence and Compo 1998) of age-detrended LDGI curves (*1*). *B*, *Chthamalus fissus*, ST11-A7. *C*, *Chione fluctifraga*, ST11-A2L. Morlet function with wave number 6 was used for wavelet transformation: *solid line* = real; *dashed line* = imaginary. *2*, Wavelet transforms reveal distinct spectral power at ca. 14 LDGIs, suggesting a fortnightly periodicity of LDGI widths. The weaker power is also visible at about 28–29 LDGIs. The contour levels are chosen so that 75%, 50%, 25%, and 5% of the wavelet power is above each level, respectively. The cross-hatched region refers to the cone of influence, where zero padding has reduced the variance. *3*, Global wavelet power spectrum.

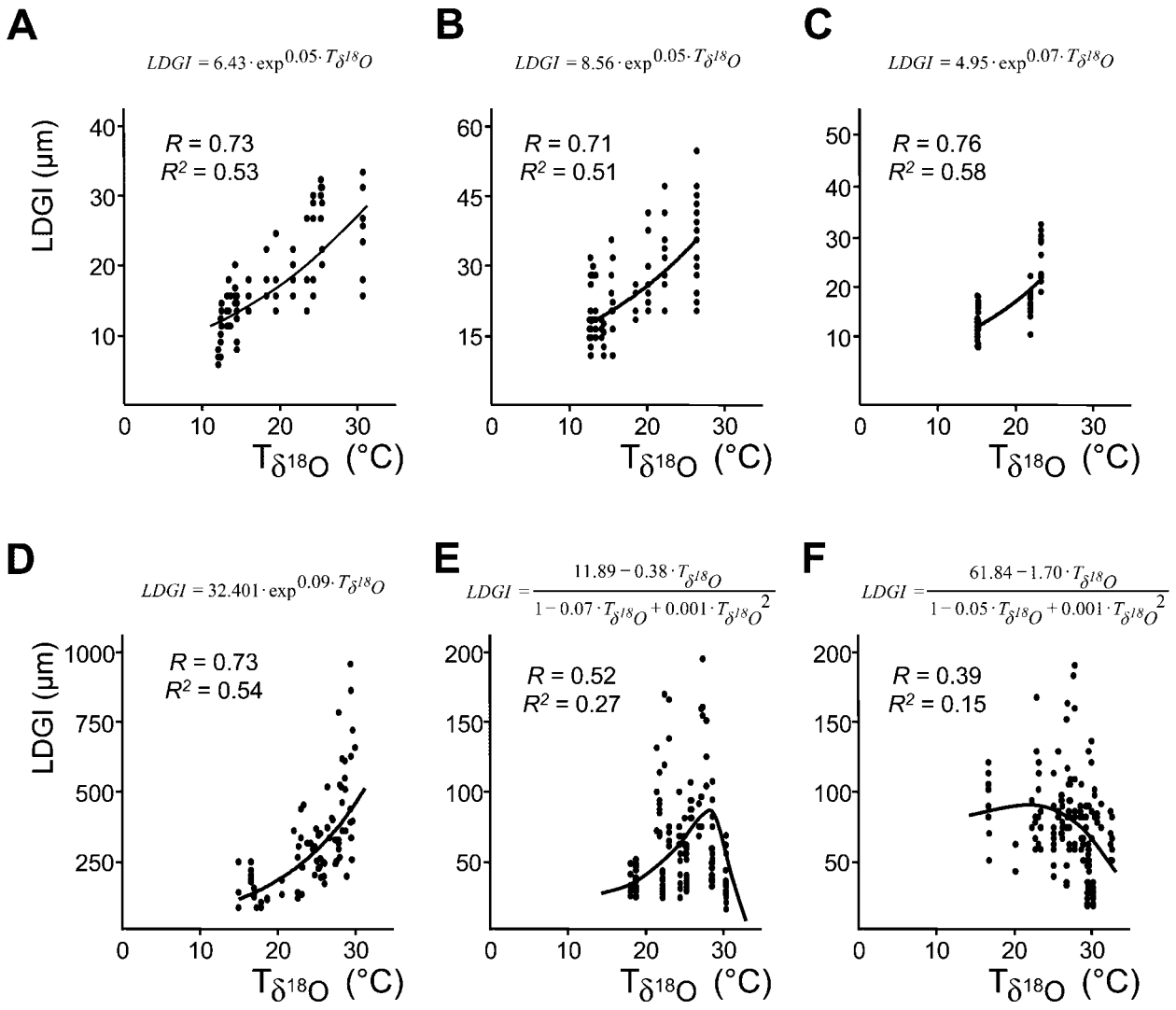

Figure 8. Growth-temperature plots. Lunar daily shell growth correlates well with shell oxygen-isotope-derived temperature. Logarithmic functions describe this relation in the case of *Chthamalus fissus* (*A*, ST11-A6; *B*, ST11-A7; *C*, ST11-A8) and *Mytella guyanensis* (*D*, ST11-A5L). However, a rational function was used for *Chione fluctifraga* (*E*, ST11-A2L; *F*, ST11-A3L). Note that maximum shell growth in the mytiloid bivalve and in the barnacles occurred at almost the highest temperatures, while the veneroid bivalve grew preferably at about 24°–27°C.

and the resulting temperature record in shell oxygen isotopes.

Another limitation of the current study originates from the low ontogenetic age of the studied organisms. Skeletons of the barnacles and the mussel started growing during the temperature-logging experiment. A full annual record of shell growth is thus not available for these two species. It remains unclear when during the year *M. guyanensis* typically starts growing, whether *C. fissus* produces shell carbonate during a hot summer, or which maximum temperatures its shell may record. On the basis of the observation that winter temperatures were overestimated, it seems reasonable to assume that actual hot summer temperature extremes will not be faithfully recorded by the barnacle either.

The effect of different ontogenetic age on skeletal growth was not taken into consideration. Here, we compared 2- and 3-yr-old shell portions of *C. fluctifraga* with those of barnacles and a mussel less than 1 yr old. Younger specimens of *C. fluctifraga* were not found near the logger. Previous studies suggested that shutdown temperatures

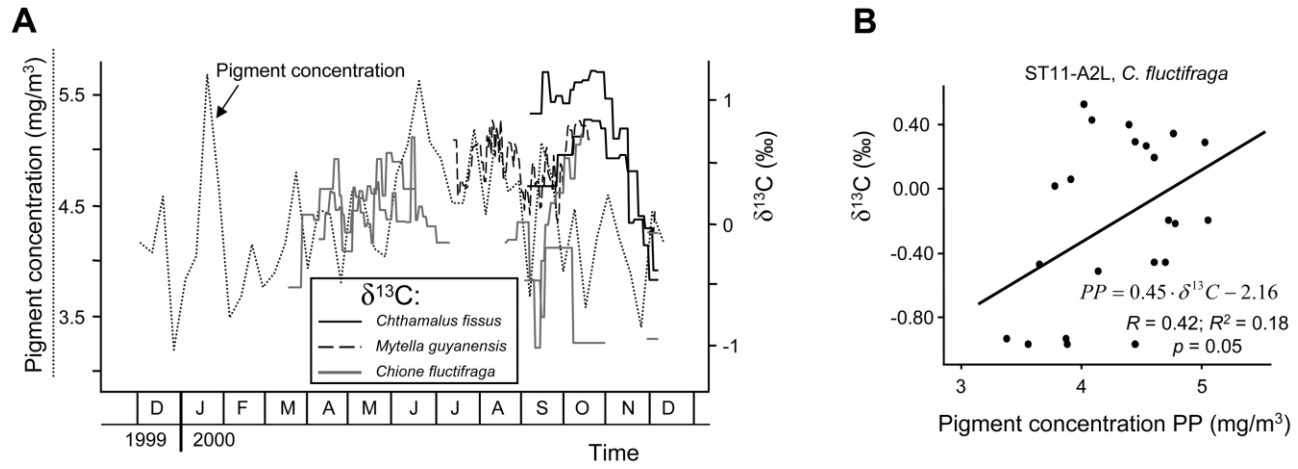

Figure 9. Shell carbon isotopes and weekly primary productivity (PP). *A*, Despite among-species differences, shell $\delta^{13}C$ curves showed some common trends that largely follow those of the chlorophyll *a* concentration. A weak linear correlation exists between weekly PP and weekly averaged $\delta^{13}C$ values of the shells (e.g., *Chione fluctifraga*, ST11-A2L [*B*]).

may change during a lifetime and may result in a reduction of the length of the growing season (Goodwin et al. 2001; Schöne et al. 2003). Our results, however, have not revealed significant differences in the number of LDGIs in the two *C. fluctifraga* shells. Perhaps duration and timing of the growing season remain unchanged—at least during youth—with strongly reduced shell growth during portions of the year when environmental conditions were suboptimal for the organism. Growth rates might have been strongly reduced and individual growth increments not discernible. This hypothesis cannot yet be confirmed, but neither can the hypothesis on shorter growing seasons of older specimens.

Possible Additional Environmental Proxies: Growth Rates, Carbon Isotopes. Variation in growth rates and shell carbon isotopes may yield additional environmental proxies for temperature and primary productivity, respectively. A close causal relationship between shell growth and temperatures has been found for many organisms (Henderson 1929; Loosanoff 1939; Loosanoff et al. 1951; Kennish and Olsson 1975; Jones 1981; Mutvei et al. 1994; Weidman et al. 1994; Bauer and Wächtler 2001). This study confirmed such results. Temperature and daily shell growth rates of all studied species were significantly correlated although weakly in the case of *C. fluctifraga*. After correction for growth trends related to ontogenetic aging, LDGI widths may function as an independent archive for reconstruction water temperature that prevailed during shell growth (Schöne et al. 2002*b*). However, such models were beyond the scope of this study and would require additional sample material of each species.

Understanding the carbon isotope system may be more difficult. According to Krantz et al. (1987), shell $\delta^{13}C$ values can potentially be used to reconstruct the primary productivity. This hypothesis is supported by two findings, namely, (1) the gross similarity between the shell $\delta^{13}C$ curves of different taxa during spring and summer, suggesting a common external forcing of the carbon isotopes, and (2) the positive correlation between shell $\delta^{13}C$ values and pigment concentration. However, variation in shell carbon isotopes during the second part of the year after the hot summer remains unexplained. From September to December, carbon isotope values varied greatly among different species and were not correlated with chlorophyll *a* levels. Numerous previous studies have identified a variety of different factors that potentially influence shell $\delta^{13}C$ values, such as the carbon isotope ratio of dissolved inorganic carbon (Mook and Vogel 1968; Andreasson and Schmitz 1998; but see Putten et al. 2000), kinetic fractionation (Owen et al. 2002), metabolic uptake (Borchardt 1985; Tanaka et al. 1986), and effects of growth rates (Lorrain et al. 2004). At present, we have no clear-cut explanation for the disagreement among the carbon isotope curves after the hot summer. Further detailed analyses combining sclerochronological and geochemical approaches might help resolve the $\delta^{13}C$ puzzle.

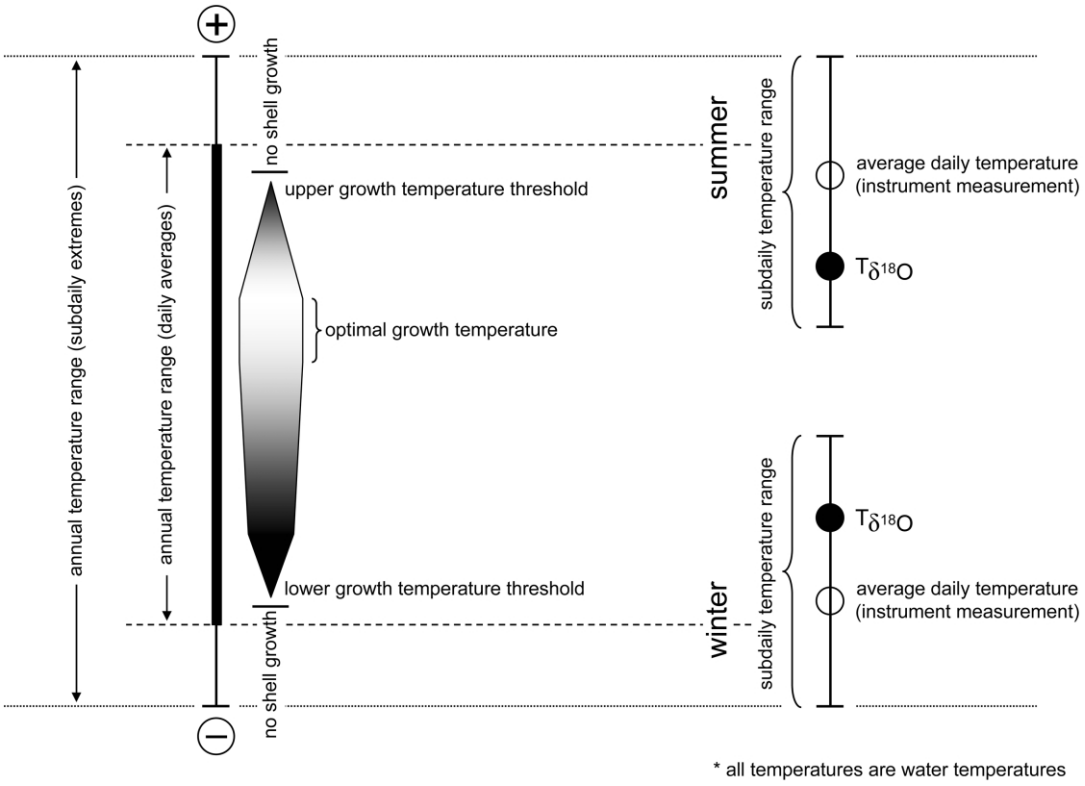

Figure 10. Model for environmental records (temperature) in accretionary biogenic skeletons. Shell growth occurs preferentially at a species-specific optimal growth temperature and only within certain temperature limits. This may prevent recognition of subdaily temperature extremes. During the hottest part of the summer, shell-derived $T_{\delta^{18}O}$ underestimates the average daily temperature. During winter, actual water temperatures are overestimated. Environmental records are biased toward optimal growth temperatures.

Conclusions

Environmental reconstructions can greatly benefit from combined analysis of proxy records from different taxa. This study demonstrated that for the biggest part of the year, water temperatures in the northern Gulf of California can be reconstructed to the nearest day and with an average precision of better than 1°C by using sclerochronologically calibrated oxygen isotope records preserved in the skeletons of barnacles, clams, and a mussel. A combined sclerochronological and isotope geochemical approach enables precise analyses of the temperature slopes (timing and duration of seasonal temperature increase and decrease) during the growing season and evaluation of day-to-day temperature differences. However, seasonal environmental extremes cannot be directly determined from the skeletal record because the shells grow at very low rates (or not at all) under suboptimal environmental conditions. Subdaily shell growth rates determined the time averaging of samples taken from shell carbonate. Because growth of these species is biased toward optimal temperatures (which differ among species), the environmental proxy record preserved in their skeletons is inherently biased toward these optima and must be interpreted with care. These results may well apply to proxy records preserved in the biogenic hard parts of all species and must be taken into consideration in future studies.

Further important results are summarized as follows: (1) The bivalve mollusks *Chione fluctifraga* and *Mytella guyanensis* and the barnacle *Chthamalus fissus* form lunar daily and fortnightly growth patterns in their skeletons, enabling a precise calendar dating of each shell portion. (2) Growing periods differed in all studied species. *Mytella guyanensis* was the only species that grew during the hottest part of the summer, and *C. fissus* was the only species that grew without interruption during the cold winter season. (3) Gaps in the record of one species can be covered by records of another species. Combining the growth or isotope records

of all species enables verification and validation of individual environmental reconstructions. (4) A bias toward maximum shell growth and species-specific optimum growth temperatures was observed, particularly during seasonal extremes. Summer temperatures were underestimated by shell $\delta^{18}O$ values, while winter temperatures were overestimated. (5) Despite higher ambient water temperatures, all three studied species recorded maximum temperatures of about 30.9°C in shell $\delta^{18}O$ values. (6) Bivalves exhibit winter shutdown temperatures of 14.2°C (*M. guyanensis*) and 15°C (*C. fluctifraga*). (7) Shell growth and temperatures are positively correlated with each other (27% of *C. fluctifraga*, 54% of *M. guyanensis*, and 58% of *C. fissus* explained variability). (8) Carbon isotopes of the studied species showed common trends that covary weakly with primary productivity; discrepancies of up to 2‰ occurred in some contemporary shell portions.

For greatest validity, paleoenvironmental and paleoclimate studies should employ a multitaxon approach and should use sclerochronological and geochemical techniques in combination. Care must be applied when interpreting actual temperature ranges from biogenic carbonates. Shell oxygen-isotope-derived temperature records may be biased toward optimum growth temperatures and the fastest skeletal growth rates. The results achieved here can supplement and improve models that aim to reconstruct true temperature extremes from incomplete or biased paleoenvironmental records (Ivany et al. 2003).

ACKNOWLEDGMENTS

We thank B. Lofgren (University of Arizona) for calculating the tidal calendar for the study area. Skin temperature (air and water temperature) data were provided by the NOAA Cooperative Institute for Research in Environmental Sciences Climate Diagnostics Center, Boulder, Colorado, from its Web site at http://www.cdc.noaa.gov/. Pigment concentration (SeaWIFS) data were obtained from NASA Goddard Earth Sciences Data and Information Services Center at http://daac.gsfc.nasa.gov/. Suggestions made by two reviewers (G. R. Clark II, University of Kansas, and one anonymous reviewer) significantly improved the manuscript. This study has been made possible by a German Research Foundation grant (to B. R. Schöne) within the framework of the Emmy Noether Program (SCHO 793/1).

REFERENCES CITED

Abades, S.; Richardson, C. A.; and Otaíza, R. 2000. Dynamical assessment of the accretionary record in the shell of the mussel *Semimytilus algosus* from a rocky shore in Chile. Biosystems 57:163–172.

Achituv, Y.; Brickner, I.; and Erez, J. 1997. Stable carbon isotope ratios in Red Sea barnacles (Cirripedia) as an indicator of their food source. Mar. Biol. 130:243–247.

Andreasson, F., and Schmitz, B. 1998. Tropical Atlantic seasonal dynamics in the early middle Eocene from stable oxygen and carbon isotope profiles of mollusc shells. Paleoceanography 13:183–192.

Ansell, A. D. 1968. The rate of growth of the hard clam *Mercenaria mercenaria* (L.) throughout the geographic range. J. Cons. Cons. Int. Explor. Mer 31:364–409.

Barker, R. M. 1964. Microtextural variation in pelecypod shells. Malacologia 2:69–86.

Bauer, G., and Wächtler, K., eds. 2001. Ecology and evolution of the freshwater mussels Unionoidea. Berlin, Springer, 394 p.

Berry, W. B. N., and Barker, R. M. 1968. Fossil bivalve shells indicate longer month and year in Cretaceous than Present. Nature 217:938–939.

———. 1975. Growth increments in fossil and modern bivalves. *In* Rosenberg, G. D., and Runcorn, S. K., eds. Growth rhythms and the history of the Earth's rotation. New York, Wiley, p. 9–25.

Bice, K. L.; Arthur, M. A.; and Marincovich, L., Jr. 1996. Late Paleocene Arctic Ocean shallow-marine temperatures from mollusc stable isotopes. Paleoceanography 11:241–249.

Borchardt, T. 1985. Relationship between carbon and cadmium uptake in *Mytilus edulis*. Mar. Biol. 85:233–244.

Bourget, E., and Crisp, D. J. 1975. Factors affecting deposition of the shell in *Balanus balanoides* (L.). J. Mar. Biol. Assoc. U.K. 55:231–249.

Clark, G. R., II. 1979. Seasonal growth variations in shells of Recent and prehistoric specimens of *Mercenaria mercenaria* from St. Catherines Island, Georgia. Anthropol. Pap. Am. Mus. Nat. Hist. 56:161–172.

Cook, E. R., and Kairiukstis, L. A., eds. 1990. Methods of dendrochronology: applications in the environmental sciences. Dordrecht, Kluwer, 394 p.

Darwin, C. 1854. A monograph of the sub-class Cirripedia, with figures of all the species: the Balanidae (or sessile Cirripedes), the Verrucidae, etc. London, Ray Society, 684 p.

de Lamarck, J. B. P. 1819. Histoire naturelle des animaux sans vertèbres. Paris, Verdière, 343 p.

Epstein, S.; Buchsbaum, H.; Lowenstam, H.; and Urey, C. 1953. Revised carbonate-water isotopic temperature scale. Geol. Soc. Am. Bull. 64:1315–1326.

Evans, J. W. 1972. Tidal growth increments in the cockle *Clinocardium nuttalli*. Science 176:416–417.

Goodwin, D. H.; Flessa, K. W.; Schöne, B. R.; and Dettman, D. L. 2001. Cross-calibration of daily growth increments, stable isotope variation, and temperature in the Gulf of California bivalve mollusk *Chione cortezi*: implications for paleoenvironmental analysis. Palaios 16:387–398.

Goodwin, D. H.; Schöne, B. R.; and Dettman, D. L. 2003. Resolution and fidelity of oxygen isotopes as paleotemperature proxies in bivalve mollusk shells: models and observations. Palaios 18:110–125.

Gould, A. A. 1850. Shells from the United States Exploring Expedition. Proc. Boston Soc. Nat. Hist. 3:292–296.

Grossman, E. L., and Ku, T. L.1986. Oxygen and carbon isotope fractionation in biogenic aragonite: temperature effects. Chem. Geol. 59:59–74.

Hall, C. A., Jr.; Dollase, W. A.; and Corbató, C. E. 1974. Shell growth in *Tivela stultorum* (Mawe, 1823) and *Callista chione* (Linnaeus, 1758) (Bivalvia): annual periodicity, latitudinal differences, and diminution with age. Palaeogeogr. Palaeoclimatol. Palaeoecol.15:33–61.

Henderson, J. T. 1929. Lethal temperatures of Lamellibranchiata. Contrib. Can. Biol. Fish. 4:399–411.

Hickson, J. A.; Johnson, A. L. A.; Heaton, T. H. E.; and Balson, P. S. 1999. The shell of the queen scallop *Aequipecten opercularis* (L.) as a promising tool for palaeoenvironmental reconstruction: evidence and reasons for equilibrium stable-isotope incorporation. Palaeogeogr. Palaeoclimatol. Palaeoecol. 154:325–337.

Ivany, C. L.; Wilkinson, B. H.; and Jones, D. S. 2003. Using stable isotopic data to resolve rate and duration of growth throughout ontogeny: an example from the surf clam, *Spisula solidissima*. Palaios 18:126–137.

Jones, D. S. 1981. Annual growth increments in shells of *Spisula solidissima* record marine temperature variability. Science 211:165–167.

Jones, D. S., and Quitmyer, I. R. 1996. Marking time with bivalve shells: oxygen isotopes and season of annual increment formation. Palaios 11:340–346.

Jones, P. D.; Osborn, T. J.; and Briffa, K. R. 2001. The evolution of climate over the last millennium. Science 292:662–667.

Kennish, M. J., and Olsson, R. K. 1975. Effects of thermal discharges on the microstructural growth of *Mercenaria mercenaria*. Environ. Geol. 1:41–64.

Khim, B.-K.; Woo, K. S.; and Je, J.-G. 2000. Stable isotope profiles of bivalve shells: seasonal temperature variations, latitudinal temperature gradients and biological carbon cycling along the east coast of Korea. Cont. Shelf Res. 20:843–861.

Kiktev, D.; Sexton, D. M. H.; Alexander, L.; and Folland, C. K. 2003. Comparison of modeled and observed trends in indices of daily climate extremes. J. Climate 16:3560–3571.

Killingley, J. W., and Newman, W. A. 1983. O-18 fractionation in barnacle calcite: a barnacle paleotemperature equation, J. Mar. Res. 40:893–902.

Klein Tank, A. M. G., and Können, G. P. 2003. Trends in indices of daily temperature and precipitation extremes in Europe, 1946–99. J. Climate 16:3665–3680.

Klein Tank, A. M. G.; Können, G. P.; and Selten, F. M. 2005. Signals of anthropogenic influence on European warming as seen in the trend patterns of daily temperature variance. Int. J. Climatol. 25:1–16.

Krantz, D.; Jones, D.; and Williams, D. 1987. Ecological and paleoenvironmental information using stable isotope profiles from living and fossil mollusks. Palaeogeogr. Palaeoclimatol. Palaeoecol. 58:249–266.

Lavín, M. F., and Sánchez, S. 1999. On how the Colorado River affected the hydrography of the upper Gulf of California. Cont. Shelf Res. 19:1545–1560.

Linnaeus, C. 1758. Systema naturae. Vol. 1. Holmiae. 10th ed. Stockholm, Laurentii Salvii. 824 p.

Loosanoff, V. L. 1939. Effect of temperature upon shell movements of clams, *Venus mercenaria* (L.). Biol. Bull. (Woods Hole) 76:171–182.

Loosanoff, V. L.; Miller, W. S.; and Smith, P. B. 1951. Growth and setting of larvae of *Venus mercenaria* in relation to temperature. J. Mar. Res. 10:59–81.

Lorrain, A.; Paulet, Y. M.; Chavaud, L.; Dunbar, R.; Mucciarone, D.; and Fontugne, M. 2004. $\delta^{13}C$ variation in scallop shells: increasing metabolic carbon contribution with body size. Geochim. Cosmochim. Acta 68: 3509–3519.

Marsh, R.; Petrie, B.; Weidman, C. R.; Dickson, R. R.; Loder, J. W.; Hannah, C. G.; Frank, K.; and Drinkwater, K. 1999. The 1882 tilefish kill: a cold event in shelf waters off the northeastern United States? Fish. Oceanogr. 8:39–49.

Mook, W. G., and Vogel, J. C. 1968. Isotopic equilibrium between shells and their environment. Science 159: 874–875.

Mutvei, H.; Westermark, T.; Dunca, E.; Carell, B.; Forberg, S.; and Bignert, A. 1994. Methods for the study of environmental changes using the structural and chemical information in molluscan shells. Bull. Mus. Oceanogr. Monaco 13:163–186.

Ohno, T. 1989. Palaeotidal characteristics determined by micro-growth patterns in bivalves. Palaeontology 32: 237–263.

Owen, R.; Kennedy, H.; and Richardson, C. 2002. Isotopic partitioning between scallop-shell calcite and seawater: effect of shell-growth rate. Geochim. Cosmochim. Acta 66:1727–1737.

Palmer, J. D.; Williams, B. G.; and Dowse, H. B. 1994. The statistical analysis of tidal rhythms: tests of the relative effectiveness of five methods using model simulations and actual data. Mar. Behav. Physiol. 24: 165–182.

Pannella, G. 1976. Tidal growth patterns in Recent and fossil mollusk bivalve shells: a tool for the reconstruction of paleotides. Naturwissenschaften 63:539–543.

Pannella, G., and MacClintock, C. 1968. Biological and environmental rhythms reflected in molluscan shell growth. Paleontol. Soc. Mem. 42:64–81.

Putten, E. V.; Dehairs, R.; Keppens, E.; and Baeyens, W. 2000. High resolution distribution of trace elements in the calcite shell layer of modern *Mytilus edulis*:

environmental and biological controls. Geochim. Cosmochim. Acta 64:997–1011.
Rhoads, D. C., and Lutz, R. A. 1980. Skeletal growth of aquatic organisms: biological records of environmental change. Top. Geobiol. 1:1–750.
Richardson, C. A.; Crisp, D. J.; and Runham, N. W. 1980. An endogenous rhythm in shell deposition in *Cerastoderma edule*. J. Mar. Biol. Assoc. U.K. 60:991–1004.
———. 1981. Factors influencing shell deposition during a tidal cycle in the intertidal bivalve *Cerastoderma edule*. J. Mar. Biol. Assoc. U.K. 61:465-476.
Rosenberg, G. D., and Runcorn, S. K. 1975. Growth rhythms and the history of the Earth's rotation. New York, Wiley, p. 9–25.
Schöne, B. R.; Dunca, E.; Fiebig, J.; and Pfeiffer, M. 2005*a*. Mutvei's solution: an ideal agent for resolving microgrowth structures of biogenic carbonates. Palaeogeogr. Palaeoclimatol. Palaeoecol. 228:149–166.
Schöne, B. R.; Fiebig, J.; Pfeiffer, M.; Gleß, R.; Hickson, J.; Johnson, A. L. A.; Dreyer, W.; and Oschmann, W. 2005*b*. Climate records from a bivalved Methuselah (*Arctica islandica*, Mollusca; Iceland). Palaeogeogr. Palaeoclimatol. Palaeoecol. 228:130–148.
Schöne, B. R.; Flessa, K. W.; Dettman, D. L.; Goodwin, D. H.; and Roopnarine, P. D. 2002*a*. Sclerochronology and growth of the bivalve mollusks *Chione fluctifraga* and *C. cortezi* in the northern Gulf of California, Mexico. Veliger 45:45–54.
Schöne, B. R.; Lega, J.; Flessa, K. W.; Goodwin, D. H.; and Dettman, D. L. 2002*b*. Reconstructing daily temperatures from growth rates of the intertidal bivalve mollusk *Chione cortezi* (northern Gulf of California, Mexico). Palaeogeogr. Palaeoclimatol. Palaeoecol. 184: 131–146.
Schöne, B. R.; Tanabe, K.; Dettman, D. L.; and Sato, S. 2003. Environmental controls on shell growth rates and $\delta^{18}O$ of the shallow-marine bivalve mollusk *Phacosoma japonicum* in Japan. Mar. Biol. 142:473–485.
Sowerby, G. B., II. 1853. Monograph of the genus *Venus*. *In* Sowerby, G. B., II, ed. Thesaurus conchyliorum; or, monographs of genera of shells. Vol. 2. London, Sowerby, p. 703–762.
Tanabe, K. 1988. Age and growth rate determinations of an intertidal bivalve, *P. japonicum*, using internal shell increments. Lethaia 21:231–241.
Tanabe, K., and Oba, T. 1988. Latitudinal variation in shell growth patterns of *P. japonicum* (Bivalvia: Veneridae) from the Japanese coast. Mar. Ecol. Prog. Ser. 47:75–82.
Tanaka, N.; Monaghan, M. C.; and Rye, D. M. 1986. Contribution of metabolic carbon to mollusk and barnacle shell carbonate. Nature 320:520–523.
Torrence, C., and Compo, G. P. 1998. A practical guide to wavelet analysis. Bull. Am. Meteorol. Soc. 79:61–78.
Tripati, A.; Zachos, J.; Marincovich, L., Jr.; and Bice, K. 2001. Late Paleocene Arctic coastal climate inferred from molluscan stable and radiogenic isotope ratios. Palaeogeogr. Palaeoclimatol. Palaeoecol. 170:101–113.
Wefer, G., and Berger, W. H. 1991. Isotope paleontology: growth and composition of extant calcareous species. Mar. Geol. 100:207–248.
Weidman, C. R.; Jones, G. A.; and Lohmann, K. C. 1994. The long-lived mollusc *Arctica islandica*: a new paleoceanographic tool for the reconstruction of bottom temperatures for the continental shelves of the northern North Atlantic Ocean. J. Geophys. Res. 99:18,305–18,314.
Wells, J. W. 1963. Coral growth and geochronometry. Nature 9:948–950.
Wurster, C. M., and Patterson, W. P. 2001. Seasonal variation in stable oxygen and carbon isotope values recovered from modern lacustrine freshwater molluscs: paleoclimatological implications for sub-weekly temperature records. J. Paleolimnol. 26:205–218.
Zakharov, Y. D.; Smyshlyaeva, O. P.; Tanabe, K.; Shigeta, Y.; Maeda, H.; Ignatiev, A. V.; Velivetskaya, T. A.; et al. 2005. Seasonal temperature fluctuations in the high northern latitudes during the Cretaceous Period: isotopic evidence from Albian and Coniacian shallow-water invertebrates of the Talovka River Basin, Koryak Upland, Russian Far East. Cretac. Res. 26:113–132.